

THE CORRELATION OF LIQUEFACTION WITH EXCESS PORE WATER PRESSURE IN LANGKAT, NORTH SUMATRA

Izzatul Aini^{1*}, Wahyu Wilopo², Teuku Faisal Fathani³

^{1,3} Department of Civil and Environmental Engineering, Universitas Gadjah Mada, Indonesia

²Department of Geological Engineering, Universitas Gadjah Mada, Indonesia

*Corresponding Author, Received: 26 Sep. 2023, Revised: 21 Feb. 2024, Accepted: 22 Feb. 2024

ABSTRACT: An earthquake is a natural occurrence that has the potential to trigger liquefaction. In fine sandy soil layers with a shallow water table, earthquakes can cause a rapid increase in excess pore water pressure (PWP), compromising the soil's effective strength and increasing the risk of liquefaction. According to the Indonesian Liquefaction Vulnerability Zone, North Sumatra is categorized as a liquefaction area. Langkat is one of the regencies in North Sumatra that is categorized as having a moderate liquefaction vulnerability. Therefore, Langkat was chosen as a research area to investigate liquefaction potential using pore water pressure (PWP) with empirical methods by Yegian and Vitelli (1981) and numerically using Deepsoil V7.0. The study area consists mostly of sand with shallow groundwater levels due to its proximity to rivers and high seismic zones associated with the Sumatran fault. The analysis is based on Standard Penetration Test data and laboratory tests from 2 boreholes with a depth of 30 m. The results show that full liquefaction potential exists at BH 01, a depth of 9–11 m below the ground surface with $r_u > 0.8$ and a limit of $\gamma_{max} \geq \gamma$. Marginal liquefaction occurs at BH 02 at a depth of 3.5 m with $r_u > 0.8$ and $\gamma_{max} < \gamma_{limit}$. Evaluation of the excess pore water pressure ratio in area prone to liquefaction is important because this condition can cause rapid damage. The low bearing capacity of the building foundation is proven by the r_u value approaching 0.8.

Keywords: Liquefaction Potential, Site response analysis, Factor of Safety, Deepsoil V7.0, PWP ratio

1. INTRODUCTION

Sumatra is situated in a high seismic zone, originating from the Sumatra or Semangko fault. The fault extends approximately 1,900 km from Banda Aceh to Semangko Bay in South Lampung, parallel to the subduction trench/zone formed by the convergence of the Eurasian and Indo-Australian Plate [1]. The zone exhibits a degree of weakness, leading to its susceptibility to shearing during earthquakes. In northern Sumatra, a significant frequency of earthquakes on land, with a magnitude of 6 to 6.9 M_w , has been observed [2]. Several studies identified earthquake and soil conditions as the triggering factors for liquefaction.

Liquefaction is a phenomenon of increasing pore water pressure which causes sandy soil particles to separate from each other so that the effective soil stress is reduced drastically or even disappears. Liquefaction is generally caused by earthquake vibrations which trigger cyclic loads and increased pore water pressure in the soil. Liquefaction causes the soil to lose its strength and stiffness to withstand the weight of the structure. This is often experienced in response to seismic shaking or other sudden changes in pressure conditions, leading to liquid-like behavior [3]. Moreover, the seismic and geological conditions at the study site fall into the liquefaction-prone category.

According to the Indonesian Liquefaction Vulnerability Zone, North Sumatra has several areas with low to moderate liquefaction potential. One of these areas is Langkat, categorized as having a moderate liquefaction vulnerability, located on the northern side of Sumatra Island [4]. Based on the geotechnical survey, the soil layers at the study site of Langkat, North Sumatra, consist of loose to dense sands with a depth of up to 30 m. The area also has high groundwater table levels due to its proximity to the Wampu River. Due to its conditions, evaluating liquefaction potential in this area is important.

A preliminary study on liquefaction potential was conducted through empirical analysis using Standard Penetration Test (SPT) data [5,6,7]. The primary concept of empirical analysis entails comparing the Cyclic Resistance Ratio (CRR) and Cyclic Stress Ratio (CSR). CRR represents the ratio of soil cyclic resistance to withstanding cyclic shear stress during the earthquake, while CSR is the shear stress induced by the earthquake or the energy released to trigger liquefaction [5].

A recent nonlinear site response analysis assessed the liquefaction potential triggered by PWP development. The change in the state of solid granular material to a liquid is caused by an increase in pore water pressure (PWP) and a decrease in effective stress. A previous study showed that the decrease in effective stress in

sediments was influenced by the excess PWP ratio (r_u) [8].

Parametric site response analysis is often carried out using the nonlinear site response analysis with PWP generation. Nonlinear effective stress analysis is affected by specific variables, such as shear modulus, soil profile, and groundwater table depth in ground motion propagation [8, 9]. The results of nonlinear site response analysis with PWP generation are proposed as criteria for the excess PWP ratio (r_u).

Based on previous results, there are no studies on liquefaction caused by excess PWP at the location. This research aims to provide insight into the potential for liquefaction due to excess PWP in Langkat, North Sumatra. In addition, the excess pore water pressure ratio obtained from the analysis is compared with the predicted value calculated from empirical data. The results will provide engineers with a better understanding of understanding and mitigating high PWP in North Sumatra.

2. STUDY SIGNIFICANCE

This study focused on identifying liquefaction potential through nonlinear site response analysis of the influence of the excess PWP ratio (r_u) in Langkat, using the open-source software Deepsoil V7.0 with the GQ/H+PWP model. Then, the excess pore water pressure ratio obtained from the analysis is compared with the predicted value calculated from empirical data. The results will provide engineers with a better understanding and mitigation of high PWP in North Sumatra.

3. SITE ANALYSIS

3.1 Study Area

This study was conducted in Langkat, North Sumatra, Indonesia, as part of the Binjai–Langsa Toll Road section. This section was one of the government's priority projects aimed at supporting national economic growth, implementing the Masterplan for Acceleration and Expansion of Indonesian Economic Development 2010–2025, and promoting the development of areas in Sumatra Island through the construction of the Trans-Sumatra Toll Road [10]. The planned construction of a connecting bridge for the toll road at this location underscored the importance of infrastructure development in the region, which was closely tied to the risk of disasters. Fig. 1 shows the distribution of borehole location. Soil drilling was carried out at 2 locations, and the N -SPT values obtained from the 2020 soil investigation were used in this study.

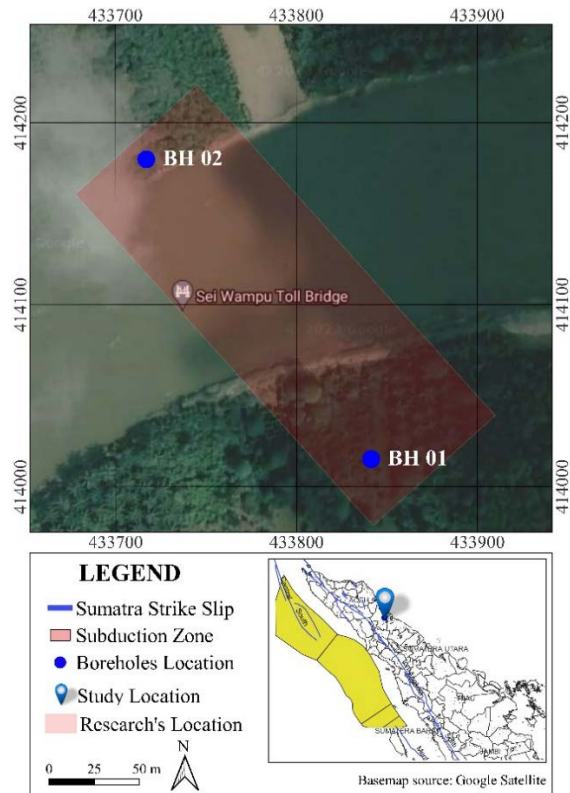


Fig. 1 Study site (Source: QGIS Software)

3.2 Geological and Geotechnical Condition

The geological conditions in the study site Langkat Regency consisted of Alluvium rock formations (Qh), comprising gravel, sand, and clay, classified as quaternary sediments (Holocene) [11]. Quaternary sediments were generally loose, decomposed, soft, and less compact. Newly deposited soil tended to be more susceptible to liquefaction than those deposited for an extended period [7].

Fig. 2 shows the soil profile and SPT results interpretation at two borehole locations. Loose sand layers were found at a depth of 6–20 m, and at a depth of 20–30 m below, the soil was relatively hard, as indicated by an average N -SPT value exceeding 50. The average N -SPT value of < 20 at the locations suggested vulnerability to liquefaction with a high potential for structural damage [12]. This study applied a groundwater table value equal to 0 or in the worst-case condition due to the proximity of the area to the river.

The shear wave velocity for site class determination was based on V_{s30} data downloaded from the United States Geological Survey (USGS) database. According to [13], the location fell under the medium soil site class (D) if V_{s30} is less than 350 m/s and more than 175 m/s. The V_{s30} data is required for the nonlinear analysis of site response.

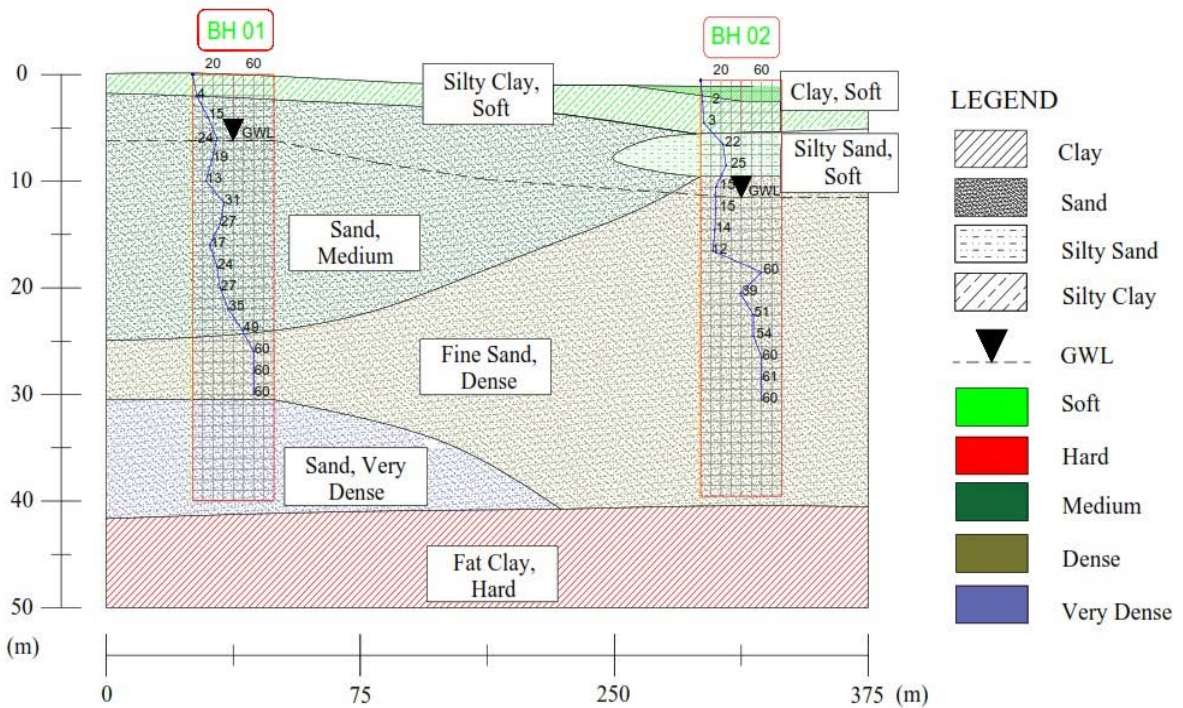


Fig. 2 Soil layer interpretation

4. METHODOLOGY

One method of evaluating liquefaction potential is to use Insitu Test data, one of which is *N-SPT* data. Empirical analysis is still the most preferred method for determining liquefaction potential in engineering practice. The main concept of this method is to compare the Cyclic Resistance Ratio (CRR) based on the value of soil resistance to liquefaction and the Cyclic Stress Ratio (CSR) based on the peak ground acceleration at the location, which is reviewed to obtain the Factor of Safety (FS) value against liquefaction calculated according to Idriss and Boulanger (2014) [14]. Equation 1–2 is used to obtain the FS value, if the Factor of Safety (FS) value is <1 then it can be concluded that there is potential for liquefaction at that location.

Then, FS is used to estimate the excess pore air

pressure ratio (r_u). Yegian and Vitteli (1981) confirmed the correlation between FS and r_u using Equation 3 [15].

$$r_u = \frac{2}{\pi} \arcsin\left(\frac{1}{FS}\right)^{\frac{1}{2\alpha\beta}} \quad (3)$$

where $CRR_{M=7.5,\sigma'vc=1}$ is cyclic resistance ratio, $(N_1)_{60cs}$ is the correction factor of fines content, K_σ is a factor correction of overburden. $CSR_{M=7.5,\sigma'vc=1}$ is cyclic stress ratio. MFS is magnitude scaling factor, K_σ is overburden correction factor. σ_{vc} is the total vertical stress, σ'_{vc} is the effective vertical stress r_d is the stress reduction coefficient, and a_{max} is the maximum peak ground acceleration. r_u is excess pore pressure ratio, α and β are constants of 0.17 and 0.19, respectively.

$$FS = \frac{CRR_{M=7.5,\sigma'vc=1}}{CSR_{M=7.5,\sigma'vc=1}} \quad (1)$$

$$FS = \frac{\exp\left(\frac{(N_1)_{60cs}}{14,1} + \left(\frac{(N_1)_{60cs}}{126}\right)^2 - \left(\frac{(N_1)_{60cs}}{23,6}\right)^3 + \left(\frac{(N_1)_{60cs}}{25,4}\right)^4 - 2,8\right)}{0,65r_d \cdot \frac{a_{max}}{g} \cdot \frac{\sigma_{vc}}{\sigma'_{vc}} \cdot \frac{1}{MFS} \cdot \frac{1}{K_\sigma}} \quad (2)$$

Numerical analysis was carried out as a comparison to empirical methods. Numerical analysis was done with 1-D *Site-Specific Response Analysis* (SSRA) using Deepsoil V7.0 software to estimate the excess pore water pressure ratio value. SSRA is the process of propagating seismic waves from the bedrock through the overlying soil layers up to the surface. The liquefaction potential is indicated to occur at a value of r_u of more than 0.8. The empirical method and Deepsoil V7.0 results can be compared to find the relationship between the increase in pore water pressure and the safety factor against liquefaction [8, 16].

Nonlinear site response analysis in one dimension (1D) was conducted in this study using the Generalized Quadratic/ Hyperbolic (GQ/H+PWP) approach. This GQ/H model could depict nonlinear characteristics of small strain and soil shear strength [17]. In this approach, the data input is unit weight (γ_{sat}), Fines Content (FC), N -SPT, V_s soil layer, and ground motion applied to each borehole. For the analysis, this study selected the strong ground motion of Niigata, Japan. The Niigata earthquake on October 23, 2004, had a magnitude of $6.6 M_w$ and affected Japan's Niigata Ken Chubu City. The primary geotechnical effects of the earthquake included landslides, liquefaction, and permanent ground displacements [18]. The ground motion of Niigata was selected due to its similarity to the largest earthquake in Langkat, which had a magnitude of $6.3 M_w$ on October 10, 1996. The Peak Ground Acceleration (PGA) of 0.39 was almost identical to the class D site of 0.32 [19]. Fig. 3 shows the ground motion of Niigata, Japan. The $6.3 M_w$ earthquake was used for empirical calculations according to the location conditions, while the $6.9 M_w$ Niigata, Japan earthquake was used for numerical calculations.

The PWP generation and dissipation model was used to consider how soil pore pressure increases and decreases during liquefaction induced by earthquakes. This model requires different input parameters for each soil layer, as indicated in Table 1.

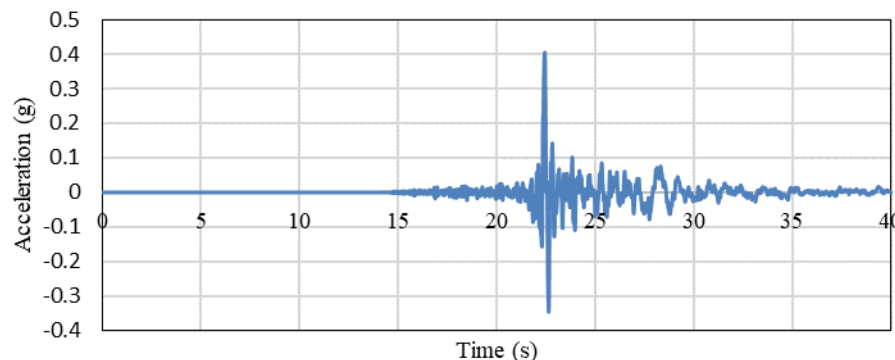


Fig. 3 The Ground Motion of Niigata, Japan

Table 1. Excess PWP Generation Model and Parameters

| PWP Model | | | | | | |
|---------------------|-----|-----|-----|----------------|-----|----------------|
| Sand | | | | | | |
| Dobry & Matasovic | | | | | | |
| f | P | F | s | γ_{typ} | v | |
| Clay | | | | | | |
| Matasovic & Vucetic | | | | | | |
| s | R | A | B | c | D | γ_{typ} |

The Vucetic & Dobry PWP model for sand is affected by the Shear Wave Velocity (V_s) and Fines Content (FC) [20] using Equations 4–5:

$$F = 3810 \times V_s^{(-1.55)} \quad (4)$$

$$s = (FC + 1)^{0.1252} \quad (5)$$

The parameter v is calculated using the correlation proposed by [20] through Equation 6:

$$v = 1 < 0.078D_r - 2.53 < 3.8 \quad (6)$$

where D_r = relative density (%). The coefficient of consolidation (c_v) for sand ranges between 0.02–0.1 m^2/s , and for clay, it is $0.00001 m^2/s$ [8]. Parameters $f=2$, $p=1$, $\gamma_{typ}=0.05$, and Max $r_u=0.95$ apply to all layers.

The Matasovic & Vucetic PWP model for clay entailed curve fitting parameters s , r , A , B , C , and D using the following equations 7–8:

$$s = 1.6374 \times PI^{(-0.802)} \times OCR^{(-0.417)} \quad (7)$$

$$r = 0.7911 \times PI^{(-0.113)} \times OCR^{(-0.417)} \quad (8)$$

The curve-fitting coefficients for the parameters are as follows: $A=7.6451$, $B=-14.714$, $C=6.38$, and $D=0.6922$ for OCR values less than 1 [17]. The input parameters for the PWP model are presented in Table 2.

Table 2. PWP Model Parameters of the Sand Layer BH 01

| Layer | Soil Type | Density | V_S (m/s) | ϕ | K_0 | c_v | s | r | A | B | C | D | γ_{tvp} |
|-------|-----------|---------|-------------|--------|-------|---------|------|------|------|--------|----------------|------|----------------|
| | | | | | | | f | p | F | s | γ_{tvp} | v | |
| 1 | Clay | Soft | 95.29 | 30.35 | 0.49 | 0.00001 | 0.31 | 0.60 | 7.65 | -14.71 | 6.38 | 0.69 | 0.05 |
| 2 | Clay | Soft | 106.76 | 30.35 | 0.49 | 0.00001 | 0.31 | 0.60 | 7.65 | -14.71 | 6.38 | 0.69 | 0.05 |
| 3 | Clay | Soft | 114.10 | 30.35 | 0.49 | 0.00001 | 0.31 | 0.60 | 7.65 | -14.71 | 6.38 | 0.69 | 0.05 |
| 4 | Clay | Soft | 119.61 | 30.35 | 0.49 | 0.00001 | 0.31 | 0.60 | 7.65 | -14.71 | 6.38 | 0.69 | 0.05 |
| 5 | Clay | Soft | 127.84 | 30.35 | 0.49 | 0.00001 | 0.31 | 0.60 | 7.65 | -14.71 | 6.38 | 0.69 | 0.05 |
| 6 | Sand | Medium | 169.68 | 38.97 | 0.37 | 0.05 | 2.00 | 1.00 | 1.33 | 1.47 | 0.05 | 3.03 | - |
| 7 | Sand | Medium | 176.72 | 38.45 | 0.38 | 0.05 | 2.00 | 1.00 | 1.25 | 1.47 | 0.05 | 2.88 | - |
| 8 | Sand | Medium | 178.34 | 38.33 | 0.38 | 0.05 | 2.00 | 1.00 | 1.23 | 1.47 | 0.05 | 2.84 | - |
| 9 | Sand | Medium | 195.40 | 41.82 | 0.33 | 0.05 | 2.00 | 1.00 | 1.07 | 1.47 | 0.05 | 3.80 | - |
| 10 | Sand | Medium | 203.10 | 41.30 | 0.34 | 0.05 | 2.00 | 1.00 | 1.01 | 1.47 | 0.05 | 3.71 | - |
| 11 | Sand | Medium | 204.87 | 38.72 | 0.37 | 0.05 | 2.00 | 1.00 | 1.00 | 1.47 | 0.05 | 2.96 | - |
| 12 | Sand | Medium | 210.58 | 38.33 | 0.38 | 0.05 | 2.00 | 1.00 | 0.95 | 1.46 | 0.05 | 2.84 | - |
| 13 | Sand | Medium | 207.68 | 34.97 | 0.43 | 0.05 | 2.00 | 1.00 | 0.97 | 1.46 | 0.05 | 1.86 | - |
| 14 | Sand | Medium | 212.01 | 34.68 | 0.43 | 0.05 | 2.00 | 1.00 | 0.94 | 1.46 | 0.05 | 1.77 | - |
| 15 | Sand | Medium | 236.07 | 42.14 | 0.33 | 0.05 | 2.00 | 1.00 | 0.80 | 1.46 | 0.05 | 3.80 | - |
| 16 | Sand | Medium | 241.28 | 41.80 | 0.33 | 0.05 | 2.00 | 1.00 | 0.77 | 1.46 | 0.05 | 3.80 | - |
| 17 | Sand | Medium | 242.68 | 40.03 | 0.36 | 0.05 | 2.00 | 1.00 | 0.77 | 1.46 | 0.05 | 3.34 | - |
| 18 | Sand | Medium | 246.99 | 39.75 | 0.36 | 0.05 | 2.00 | 1.00 | 0.75 | 1.46 | 0.05 | 3.26 | - |
| 19 | Sand | Medium | 239.67 | 35.32 | 0.42 | 0.05 | 2.00 | 1.00 | 0.78 | 1.46 | 0.05 | 1.96 | - |
| 20 | Sand | Medium | 242.94 | 35.09 | 0.43 | 0.05 | 2.00 | 1.00 | 0.76 | 1.43 | 0.05 | 1.89 | - |
| 21 | Sand | Medium | 254.67 | 37.88 | 0.39 | 0.05 | 2.00 | 1.00 | 0.71 | 1.43 | 0.05 | 2.71 | - |
| 22 | Sand | Medium | 258.08 | 37.66 | 0.39 | 0.05 | 2.00 | 1.00 | 0.70 | 1.43 | 0.05 | 2.64 | - |
| 23 | Sand | Medium | 264.45 | 38.60 | 0.38 | 0.05 | 2.00 | 1.00 | 0.67 | 1.43 | 0.05 | 2.92 | - |
| 24 | Sand | Medium | 267.74 | 38.39 | 0.38 | 0.05 | 2.00 | 1.00 | 0.66 | 1.43 | 0.05 | 2.86 | - |
| 25 | Sand | Hard | 278.23 | 41.02 | 0.34 | 0.10 | 2.00 | 1.00 | 0.62 | 1.43 | 0.05 | 3.63 | - |
| 26 | Sand | Hard | 281.81 | 40.80 | 0.35 | 0.10 | 2.00 | 1.00 | 0.61 | 1.43 | 0.05 | 3.56 | - |
| 27 | Sand | Hard | 295.16 | 45.10 | 0.29 | 0.10 | 2.00 | 1.00 | 0.57 | 1.43 | 0.05 | 3.80 | - |
| 28 | Sand | Hard | 299.08 | 44.86 | 0.29 | 0.10 | 2.00 | 1.00 | 0.55 | 1.43 | 0.05 | 3.80 | - |
| 29 | Sand | Hard | 309.18 | 47.44 | 0.26 | 0.10 | 2.00 | 1.00 | 0.53 | 1.43 | 0.05 | 3.80 | - |
| 30 | Sand | Hard | 313.24 | 47.24 | 0.27 | 0.10 | 2.00 | 1.00 | 0.52 | 1.43 | 0.05 | 3.80 | - |
| 31 | Sand | Hard | 317.13 | 47.06 | 0.27 | 0.10 | 2.00 | 1.00 | 0.51 | 1.43 | 0.05 | 3.80 | - |
| 32 | Sand | Hard | 320.87 | 46.88 | 0.27 | 0.10 | 2.00 | 1.00 | 0.50 | 1.43 | 0.05 | 3.80 | - |
| 33 | Sand | Hard | 324.48 | 46.71 | 0.27 | 0.10 | 2.00 | 1.00 | 0.49 | 1.43 | 0.05 | 3.80 | - |

5. RESULTS AND DISCUSSION

5.1 Liquefaction Potential Analysis

Liquefaction potential analysis was carried out at all boreholes at the research location using the simplified procedure method developed by Idriss and Boulanger (2014). Liquefaction potential analysis with a $6.3 M_w$ earthquake scenario determined to be the most significant earthquake between 1992–2022 within a radius of 500 km. The groundwater level uses a submerged scenario in the analysis. It was chosen to plan a conservative structural design.

The FS value used for numerical calculations for each borehole can be seen in Fig. 4. In general, liquefaction occurs at shallow depths, namely 0–20 m with FS values varying between 0.3–2. FS_{Liq} value < 1 has liquefaction potential, because the soil is unable to withstand earthquake loads, where the CRR $<$ CSR value. Liquefaction predominantly occurs in the top layer which has an N -SPT value of less than 20 and is a type of very loose to medium sandy soil [21]. The results of calculating liquefaction potential in this study are in line with the results of previous research which shows that liquefaction can occur at shallow depths [22, 16].

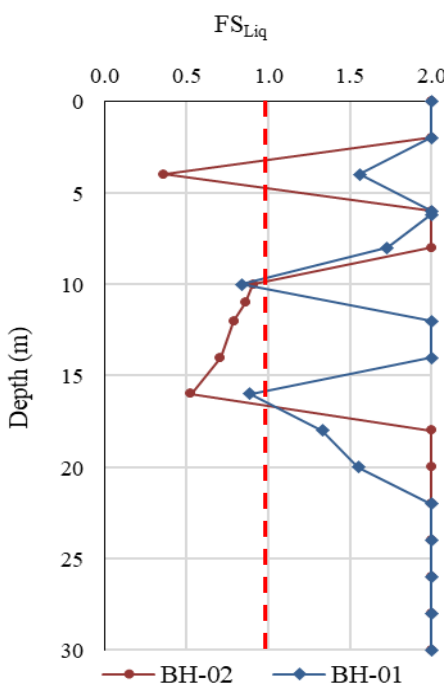


Fig. 4 FS liquefaction values in two boreholes

One of models for assessing liquefaction potential was using a nonlinear site response analysis model that considered the effect of PWP. When earthquakes occur continuously, water cannot escape through the soil pore. This led to PWP reaching its maximum condition and decreasing soil-bearing capacity. Non-linear site response research was conducted using the Deepsoil V7.0 program. Numerical integration in the time domain was employed to determine soil stiffness and damping ratio during a non-linear investigation of site reactivity. The stress-strain relationship was applied at the beginning of each time step to obtain the appropriate soil properties for that time step. To accurately follow the non-linear and inelastic stress-strain relationship, additional parameters were required to evaluate liquefaction potential through a non-linear and effective stress site response analysis, considering the accumulation and dissipation of pore water pressure.

Sand boils can occur in shallow and thick layers of sandy soil without experiencing significant strain softening, as discussed in reference [23]. This phenomenon can result in a relatively high excess porewater pressure ratio ($r_u = 0.8$). The GQ/H+PWP model can provide a realistic response for soil liquefaction where the following criteria are met the excess PWP ratio $r_u < 0.8$, and the maximum cyclic shear strain γ_{max} is less than γ_{limit} . The liquefaction was observed in the shear stress relationship-shear strain hysteresis loops when the transition was from almost hyperbolic to "banana-shaped". This hysteresis

loop exhibits significant stiffness/ dilation at higher shear strains and remains relatively flat at lower to moderate shear strains. The limit shear strain values are $\gamma_{max} = 2\%$ for loose soil ($D_r = 30\text{--}50\%$), 1.5% for moderately dense soils ($D_r = 50\text{--}70\%$), and 1.2% for dense soils ($D_r = > 70\%$), with effective stress ranging from σ'_{vo} 35 to 180 kPa. Marginal liquefaction is attained when $r_u > 0.8$ and $\gamma_{max} < \gamma_{limit}$. Full liquefaction, on the other hand, is experienced either within the range of $0.8 \leq r_u \leq 0.9$ and $\gamma_{max} \geq \gamma_{limit}$ or when $r_u > 0.9$. Non-liquefaction takes place when $r_u < 0.8$ [20].

Fig. 5 shows the r_u values obtained from borehole BH 01. The maximum r_u value in BH 01 was 0.95 in layers 13–14 at a depth of 10–11 m. According to several studies [8, 20], a r_u value greater than 0.8 indicated the occurrence of liquefaction. In layers 8–14 at a depth of 5–11 m, the r_u value reached 0.8 at different earthquake shaking times. The r_u value in layer 8 (at a depth of 5 m) reached 0.8 at 62 s of earthquake shaking, and layer 12 (at a depth of 9 m) reached 0.8 at 41 s. Meanwhile, layers 13–14 (at a depth of 10–11 m) experienced the fastest increase in the r_u value, reaching 0.8 within 24 s. Layers 7, 15, 16, 17, 18, 19, and 20 range of 0.62–0.78.

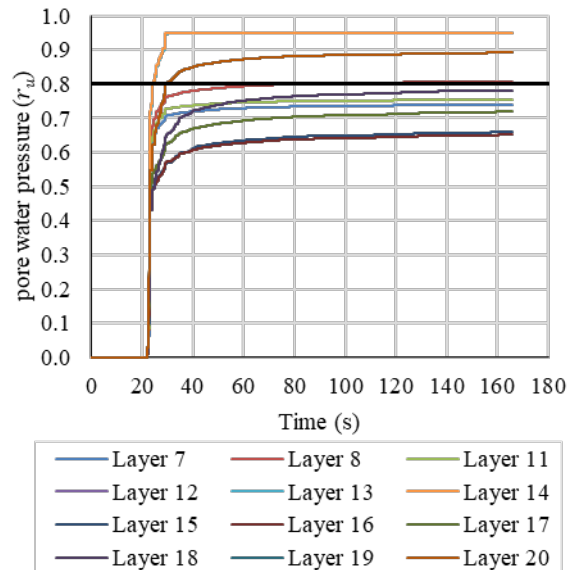


Fig. 5 PWP in Soil Layer BH 01

Fig. 6 displays the r_u values obtained from borehole BH 02. In BH 02, r_u value was 0.8 in layer 7 (at a depth of 3.5 m) and reached 0.8 at 29.6 s. Layers 10, 11, 21, 22, and 23 have a value range of 0.69–0.75. Although the resulting r_u values were less than 0.8, these layers with a r_u value range of 0.6–0.8 were indicated to have initiated the pre-liquefaction phase. However, further studies were needed to precisely understand the pre-liquefaction process [24].

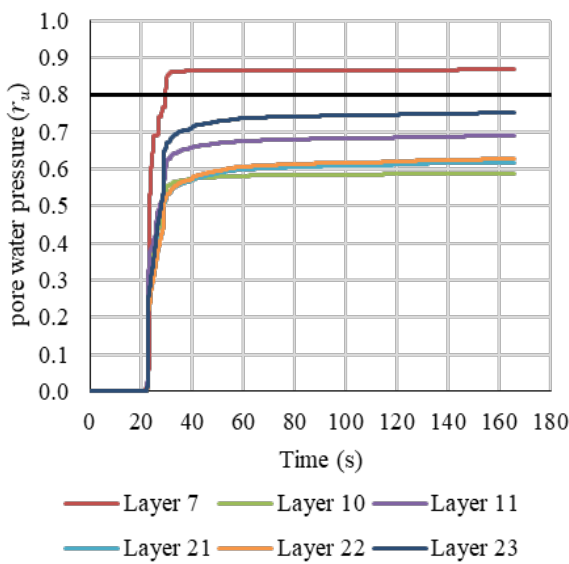


Fig. 6 PWP in Soil Layer BH 02

Table 3. Liquefaction Potential Analysis

| Layer | BH 01 | | | | | | BH 02 | | | | | | | |
|-------|-----------|-------------------------------------|-------|-----------|--------------------|----------------------|---------|-----------|-------------------------------------|-------|-----------|--------------------|----------------------|---------|
| | Depth (m) | σ'_{vo} (kN/m ²) | r_u | D_r (%) | γ_{max} (%) | γ_{limit} (%) | Remarks | Depth (m) | σ'_{vo} (kN/m ²) | r_u | D_r (%) | γ_{max} (%) | γ_{limit} (%) | Remarks |
| 1 | 0.5 | 4.23 | 0.01 | 38.90 | 0.25 | 2.0 | NL | 0.5 | 4.09 | 0.00 | 27.51 | 0.09 | 2.0 | NL |
| 2 | 1.0 | 8.47 | 0.07 | 38.90 | 0.34 | 2.0 | NL | 1.0 | 8.19 | 0.03 | 27.51 | 0.18 | 2.0 | NL |
| 3 | 1.5 | 12.70 | 0.21 | 38.90 | 0.62 | 2.0 | NL | 1.5 | 12.28 | 0.11 | 27.51 | 0.29 | 2.0 | NL |
| 4 | 2.0 | 16.94 | 0.35 | 38.90 | 1.03 | 2.0 | NL | 2.0 | 16.37 | 0.13 | 27.51 | 0.52 | 2.0 | NL |
| 5 | 3.0 | 25.40 | 0.66 | 38.90 | 0.98 | 2.0 | NL | 2.5 | 20.46 | 0.21 | 27.51 | 0.95 | 2.0 | NL |
| 6 | 4.0 | 33.21 | 0.64 | 71.28 | 0.76 | 1.5 | NL | 3.0 | 24.56 | 0.44 | 27.51 | 1.74 | 2.0 | NL |
| 7 | 4.8 | 39.45 | 0.74 | 69.31 | 0.92 | 1.5 | NL | 3.5 | 28.65 | 0.87 | 27.51 | 1.30 | 2.0 | ML |
| 8 | 5.0 | 41.01 | 0.81 | 68.85 | 0.88 | 1.5 | ML | 4.0 | 32.81 | 0.38 | 33.69 | 0.37 | 2.0 | NL |
| 9 | 6.0 | 49.89 | 0.57 | 81.99 | 0.83 | 1.2 | NL | 4.5 | 36.98 | 0.43 | 33.69 | 0.43 | 2.0 | NL |
| 10 | 7.0 | 58.76 | 0.62 | 80.04 | 1.05 | 1.2 | NL | 5.0 | 41.14 | 0.59 | 32.92 | 0.48 | 2.0 | NL |
| 11 | 8.0 | 67.04 | 0.75 | 70.33 | 1.26 | 1.2 | ML | 5.5 | 45.30 | 0.69 | 32.12 | 0.32 | 2.0 | NL |
| 12 | 9.0 | 75.32 | 0.83 | 68.86 | 3.98 | 1.5 | FL | 6.0 | 50.81 | 0.02 | 78.61 | 0.13 | 1.2 | NL |
| 13 | 10 | 82.89 | 0.95 | 56.23 | 10.01 | 1.5 | FL | 6.5 | 56.31 | 0.03 | 77.39 | 0.14 | 1.2 | NL |
| 14 | 11 | 90.46 | 0.95 | 55.15 | 7.20 | 1.5 | FL | 7.0 | 61.82 | 0.03 | 76.25 | 0.14 | 1.2 | NL |
| 15 | 12 | 100.16 | 0.66 | 83.17 | 1.10 | 1.2 | NL | 8.0 | 73.25 | 0.02 | 78.76 | 0.13 | 1.2 | NL |
| 16 | 13 | 109.87 | 0.65 | 81.92 | 1.22 | 1.2 | ML | 9.0 | 84.69 | 0.03 | 77.11 | 0.28 | 1.2 | NL |
| 17 | 14 | 119.10 | 0.72 | 75.25 | 1.27 | 1.2 | ML | 10 | 91.92 | 0.32 | 59.07 | 0.43 | 1.5 | NL |
| 18 | 15 | 128.33 | 0.78 | 74.20 | 1.67 | 1.2 | ML | 11 | 99.16 | 0.32 | 58.03 | 0.45 | 1.5 | NL |
| 19 | 16 | 136.37 | 0.89 | 57.55 | 1.88 | 1.5 | FL | 12 | 106.39 | 0.34 | 57.06 | 0.49 | 1.5 | NL |
| 20 | 17 | 144.42 | 0.77 | 56.71 | 1.52 | 1.5 | ML | 13 | 113.63 | 0.53 | 56.16 | 0.55 | 1.5 | NL |
| 21 | 18 | 153.29 | 0.81 | 67.16 | 1.32 | 1.5 | ML | 14 | 120.73 | 0.62 | 53.40 | 0.61 | 1.5 | NL |
| 22 | 19 | 162.17 | 0.80 | 66.34 | 1.20 | 1.5 | ML | 15 | 127.84 | 0.63 | 52.61 | 0.82 | 1.5 | NL |
| 23 | 20 | 171.40 | 0.66 | 69.89 | 1.12 | 1.5 | NL | 16 | 134.69 | 0.75 | 47.90 | 0.79 | 1.5 | NL |
| 24 | | | | | | | | 17 | 141.54 | 0.40 | 56.70 | 0.35 | 1.5 | NL |
| 25 | | | | | | | | 18 | 154.52 | 0.03 | 72.48 | 0.15 | 1.2 | NL |
| 26 | | | | | | | | 19 | 167.50 | 0.04 | 71.20 | 0.17 | 1.2 | NL |
| 27 | | | | | | | | 20 | 177.80 | 0.04 | 99.86 | 0.20 | 1.2 | NL |

Note: NL: No Liquefaction, FL: Full Liquefaction, ML: Marginal Liquefaction

This reduction in effective stress can lead to a loss of shear strength in the soil, making it susceptible to liquefaction when a critical level of excess pore water pressure is reached.

The analysis of liquefaction potential using PWP had also been conducted in a previous study [8] in Palu, Central Sulawesi. The location was characterized by predominantly sandy soil with a $7.5 M_w$ earthquake. The results showed that the r_u value reached 0.8 at an earthquake duration of 7.9 s. Compared to this study, where the r_u value was 0.8 at a duration of 24 s, there was a difference in time. This difference was affected by the earthquake magnitude, where a larger earthquake led to a faster increase in the r_u value.

The empirical calculation results are then compared with the numerical calculations shown in Fig. 7

In general, the liquefaction layer on BH 01 between the two methods has similar results. At a depth of 9–10 m, it shows a FS value >1 and has a r_u of 0.83–0.95 so that pore water pressure induces liquefaction.

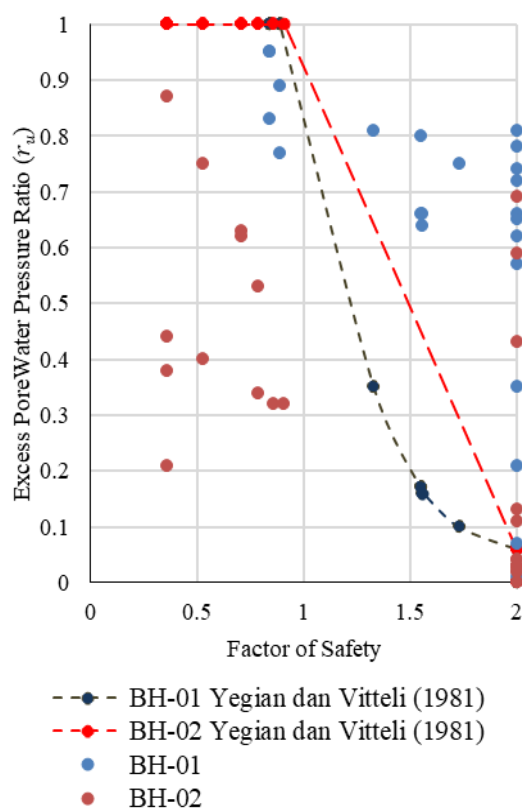


Fig. 7 FS vs. Excess pore water pressure ratio based on empirical and numerical methods

However, in BH 02, for example, at a depth of 10 m, it shows a FS value of 0.91, the r_u value obtained from empirical calculations using the method by Yegian and Vitelli (1981) is 1 but the r_u value in numerical results using software tools

produces a value of 0.32. There are differences in results between the two methods. So further control is needed because the results are not in line with numerical and empirical [22].

6. CONCLUSION

Based on the analysis that has been carried out, both boreholes have soil that has the potential for liquefaction at varying depths ranging from 0–20 m. Full liquefaction potential at the research location is at BH 01, a depth of 9–11 m below the ground surface with $r_u > 0.8$ and a limit of $\gamma_{max} \geq \gamma$. Full liquefaction can result in loss of bearing capacity and severe damage to surrounding structures. Marginal liquefaction occurs at BH 02 at a depth of 3.5 m with $r_u > 0.8$ and $\gamma_{max} < \gamma_{limit}$. For other layers, although the resulting r_u value is less than 0.8, layers with a r_u value range of 0.6–0.8 are indicated to have the potential to experience a pre-liquefaction process.

Evaluation of the excess pore water pressure ratio in areas prone to liquefaction is important because this condition can cause rapid damage. The low bearing capacity of the building foundation, as evidenced by the r_u value approaching 0.8. However, research can be conducted to accurately estimate the excess pore air pressure ratio using other methods, such as the application of laboratory soil tests or measurement of pore air pressure in the field.

7. ACKNOWLEDGMENTS

The authors are grateful to PT Hutama Karya Infrastruktur Binjai–Langsa for providing assistance and data needed in this study.

8. REFERENCES

- [1] Sieh, Kerry, and Danny Natawidjaja, Neotectonics of the Sumatran Fault, Indonesia, *Journal of Geophysical Research: Solid Earth* Vol. 105 No B12, 2000, pp. 28295–28326.
- [2] McCaffrey, R. The Tectonic Framework of the Sumatran Subduction Zone. *Annual Review of Earth and Planetary Sciences* 2009, Vol. 37, pp. 345–66.
- [3] Das Braja M., and Ramana G.V. *Principles of Soil Dynamics* 2nd. Stamford: Cengage Learning, 2011.
- [4] Ministry of Energy and Mineral Resources, *Map of Indonesia's Liquefaction Vulnerability Zone*, 2019.
- [5] Idriss I.M., and Boulanger R.W., *Soil Liquefaction During Earthquakes*, *Machinery and Production Engineering*, Univ. of California, Davis, 2008.

[6] Hakam A., and Suhelmidawati E. Liquefaction Due to the September 30, 2009, Earthquake in Padang, Procedia Engineering, Vol 54, 2013, pp. 140–146

[7] Jalil, A., Fathani, T. F., Satyarno, I., and Wilopo, W., A Study on the Liquefaction Potential in Banda Aceh City after the 2004 Sumatera Earthquake, International Journal of GEOMATE, Vol. 18, Issue 65, 2020, pp. 147–155.

[8] Jalil A., Fathani T.F., Satyarno I., & Wilopo W. Non-linear site response analysis approach to investigate the effect of pore water pressure on liquefaction in Palu, IOP Conference Series: Earth and Environmental Science, Vol. 871, Issue 1, 2021.

[9] Olson S M., Mei X., and Hashash Y M A., Nonlinear site response analysis with pore-water pressure generation for liquefaction triggering evaluation J. Geotech. Geoenvir. Eng, Vol. 146, Issue 2, 2020, pp. 1–17.

[10] Presidential Regulation Number 100 the Year 2014., Concerning the Acceleration of Toll Road Development in Sumatra. RI Cabinet Secretariat, Jakarta, Indonesia, 2014.

[11] Bennett J.D., Bridge D.McD., Cameron N.R., Djunuddin A., Ghazali S.A., Jeffery D.H., Kartawa W., Keats W., Rock N.M.S., Thomson S.J., and Whandoyo R., Geology Map of the Medan Quadrangle, Sumatera, 1981.

[12] Seed H.B., Tokimatsu, K., and Chung, R.M., Influence of SPT Procedures in Soil Liquefaction Resistance Evaluations, Journal of Geotechnical Engineering, Vol. 111, No. 12, 1985, pp. 1425–1445.

[13] National Center for Earthquake Studies: Indonesian Seismic Sources and Seismic Hazard Maps, Center for Research and Development of Housing and Resettlement. 2017.

[14] Boulanger, R. W., and Idriss, I. M., CPT and SPT Based Liquefaction Triggering Procedures, Rep. No. UCD/CGM-14/01, Univ. of California, Davis, CA, 2014.

[15] Yegian, M. K., & Vitelli, B. M., Analysis for Liquefaction: Empirical Approach, International Conferences on Recent Advances in Geotechnical Earthquake Engineering and Soil Dynamics, Int. Conf. Recent Adv. Geotech. Earthq. Eng. Soil Dyn., 1981, pp. 1–6.

[16] Mase, L. Z., Liquefaction potential analysis along coastal area of Bengkulu province due to the 2007 Mw 8.6 Bengkulu earthquake, Journal of Engineering and Technological Sciences, Vol. 49, No. 6, 2017, pp. 721-736.

[17] Hashash Y.M.A., Musgrove M.I., Harmon J.A., Ilhan O., Xing G., Numanoglu O., Groholski D.R., Phillips C.A., and Park D. DEEPSOIL 7.0, User Manual. Urbana, IL: Board of Trustees of University of Illinois at Urbana-Champaign, 2020.

[18] Scawthorn, Charles, and Ellen M. Rathje, “The 2004 Niigata Ken Chuetsu, Japan, Earthquake.” Earthquake Spectra, Vol. 22(1_suppl), 2006, pp. 1–8.

[19] Indonesian Standard Code, Earthquake Resistance Design for Buildings (SNI 03-1726-2019), National Standardization Agency, 2019.

[20] Mei X. Pore Pressure Generation and Liquefaction Analysis Using Non-linear, Effective Stress-Based Site Response Analysis, University of Illinois, Urbana-Champaign, 2018.

[21] Seed, H. B., Tokimatsu, K., and Chung, R. M., Influence of SPT Procedures in Soil Liquefaction Resistance Evaluations.Journal of Geotechnical Engineering, Vol. 111, No. 12,1985, pp. 1425-1445.

[22] Ali Z., Ahmad R., and Sito I, The Correlation of Liquefaction Potential with Excess Pore Water Pressure in Kretek 2 Bridge Area using Empirical and Numerical Methods, Journal of the Civil Engineering Forum, Vol. 10, No. 1, 2024, pp. 39-48.

[23] Kramer, S. L., Astanesh Asl, B., Ozener, P., & Sideras, S. S. Effects of Liquefaction on Ground Surface Motions. In A. Ansal & M. Sakr (Eds.), Perspectives on Earthquake Geotechnical Engineering, Springer International Publishing, Vol. 37, 2015, pp. 285–309.

[24] Khalid B. C. B., Assessment of Liquefaction Potential Using Empirical Equations and 1D Ground Response Analysis for Agartala City, Indian Geotechnical Conference 2017 GeoNEst, IIT Guwahati, India, 2017.

[25] Tohumcu Özener, P., Özaydin, K., & Berilgen, M. M., Investigation of liquefaction and pore water pressure development in layered sands, Bulletin of Earthquake Engineering, Vol. 7, No. 1, 2009, pp. 199–219.